

**GENE EXPRESSION PROFILE AND MODULATION OF
GENETIC PATHWAYS IN ACUTE MYELOID
LEUKAEMIA T(8;21)**

SALEM ALI ALSALEM BASHANFER

UNIVERSITI SAINS MALAYSIA

2013

**GENE EXPRESSION PROFILE AND MODULATION OF
GENETIC PATHWAYS IN ACUTE MYELOID
LEUKAEMIA T(8;21)**

by

SALEM ALI ALSALEM BASHANFER

**Thesis submitted in fulfillment of the requirements for the degree of
Doctor of Philosophy**

June 2013

ACKNOWLEDGEMENTS

With great pleasure I would like to express my gratitude to all who have contributed to this thesis. First and foremost I would like to thank Allah Almighty for his immense blessings and help provided to me throughout my life.

I thought it is enough to say thank you to someone helped me during my life. However, I believe now that a lifetime is not enough to thank my supervisors AP Dr. Narazah Mohd Yusoff, Prof. Mohd Saifulaman Mohd Said, and AP Dr. Rosline Hassan for believing in me even in times that I am unwilling to believe in myself. I would have been lost without all of you. Your patience, motivation, guidance, enthusiasm, and immense knowledge helped me in all the time of research and writing of this thesis. I could not have imagined having better advisors and mentors for my PhD study.

I am heartily thankful to Prof. Olaf Heidenreich at Newcastle University (UK) for his scientific advice, suggestions, knowledge and many insightful discussions through this project. I was lucky to have this collaboration.

Besides my advisors, I would like in advance to thank the rest of my thesis committee, for their encouragement, insightful comments, and hard questions.

I take this opportunity to sincerely acknowledge University Sains Malaysia (USM), Research Creativity and Management Office (RCMO), Institute of Postgraduate Studies (IPS), and Advanced Medical and Dental Institute (AMDI) for their generosity and providing several grants to accomplish this work. I also acknowledge Hodiedah University and my country Yemen for supporting my scholarship.

To the staff of IPPT, I am grateful for the chance to be a part of the lab. Thank you for welcoming me as a friend and helping me during the last five years.

I expand my thanks to the staff and students colleagues of regenerative medicine cluster specially Rohani Bakar, Faizatul Syima, Fatimah Azlina, Mohamad Basir, Abdullah Al-Alimi, Omar Saeed, Saleh Ben Amer, Emmanuel Jairaj, and Asmida Isa for providing a stimulating and fun environment. My sincere gratitude also goes to Dr. Faisal Al-Hassan for helping me during the flow cytometry experiments.

I would like to thank the staff of immunology and infectious disease clusters for allowing me to use flow cytometry and electroporator machines.

I also thank my friends at USM and UKM especially Ahmed Alrifai, Osamah Alqershi, Omar Aljunaidi, Mohamed Baobeed, Ahmed Ismael and Abdullah alwajeel for encouraging me throughout my study.

I owe my deepest gratitude to my Bachelor and Master colleagues Nashwan Nashir, Hisham Mahmoud, Mohammed Al-Attas, Mazen Alnoom, and Khaled Radman for all their support, help and for the nice time we spent together.

If I did not mention someone's name here, it does not mean that I do not acknowledge your support and help. Again, I would like to thank everyone who supported and helped me during my PhD study.

Lastly, and most importantly, I wish to thank my parents, my wife, my daughter, my son, my brother, and my sisters. To my parents, you raised me, supported me, taught me, and loved me; I owe you all my achievements, small and big victories. To my wife, I hope to be able to give you back all your love, tenderness and care that you shared with me. To my daughter Hala and my son Ahmed, I love you. To my brother and sisters, thank you for showing an excellent example of how brotherhood/sisterhood should be.

To you I dedicate this thesis.

Salem Ali Al-Salem Bashanfer

TABLE OF CONTENTS

ACKNOWLEDGEMENTS	ii
TABLE OF CONTENTS.....	iv
LIST OF TABLES.....	xi
LIST OF FIGURES.....	xii
LIST OF APPENDICES.....	xxii
LIST OF ABBREVIATIONS.....	xxvi
ABSTRAK.....	xxxiii
ABSTRACT.....	xxxvi
CHAPTER 1 Introduction.....	1
1.1 Background.....	1
1.2 Rationale of the study.....	4
1.3 General objective.....	5
1.3.1 Specific objectives.....	5
1.4 Hypothesis.....	6
1.5 Outcomes of the study.....	6
CHAPTER 2- Literature review.....	7
2.1 Epidemiology.....	7
2.2 Aetiology	8
2.3 Classification.....	9
2.3.1 AML with <i>t(8;21)</i>	13
2.3.1.1 Morphological changes and immunophenotyping.....	15
2.4 Genetic alterations in AML	16
2.4.1 Alterations involving transcription factors.....	16
2.4.1.1 Core Binding Factor (CBF).....	16

2.4.1.2 <i>t(15;17)(q22;q12)/PML-RARα</i>	16
2.4.1.3 Mixed Lineage Leukaemia (<i>MLL</i>): 11q23 Translocation.	17
2.4.1.4 C/EBP α	18
2.4.1.5 PU.1.....	19
2.4.1.6 <i>HOX</i> genes.....	20
2.4.1.7 WTI.....	20
2.4.1.8 EVI-1.....	21
2.4.1.9 C-Myb.....	21
2.4.2 Alteration of signal transduction.....	22
2.4.2.1 FLT3.....	22
2.4.2.2 c-Kit.....	23
2.4.2.3 RAS mutations.....	24
2.4.2.4 Wnt pathway.....	24
2.4.2.5 MAP kinase signalling pathways (MAPKs).....	26
2.4.2.6 JAK-STAT signalling pathway.....	30
2.4.2.7 PI3K/AKT.....	31
2.4.2.8 Notch signalling pathway.....	31
2.4.2.9 NF- κ B.....	32
2.4.2.10 Transforming Growth Factor (TGF β).....	33
2.5 AML stem cell properties.....	34
2.5.1 Phenotype.....	34
2.5.2 Cell cycle.....	34
2.5.3 Regulation of cell death and self-renewal.....	35
2.6 Apoptosis.....	35
2.7 Treatment of AML.....	37

2.7.1 Standard Therapy "3+7".....	37
2.7.2 Monoclonal Antibody Therapy.....	38
2.7.3 Stem cell transplantation.....	39
2.7.4 Haematopoietic growth factors and others differentiation therapy modes.....	39
2.7.5 Minimal Residual Disease (MDR).....	41
2.7.6 Vaccine therapy.....	42
2.8 RNA Interference.....	42
2.8.1 RNAi application in leukaemia.....	43
2.9 Microarray technology	43
2.9.1 The application of microarrays in cancer research	45
CHAPTER 3 Comparison of gene expression profiles of acute myeloid leukaemia <i>t(8;21)</i> patient samples and their corresponding cell line models.....	46
3.1 Introduction.....	46
3.2 Methodology.....	49
3.2.1 Patient, control specimens and cell line culturing.....	49
3.2.2 RNA isolation.....	49
3.2.3 RNA quality control.....	50
3.2.4 Total RNA amplification.....	51
3.2.5 Direct hybridization.....	53
3.2.6 Microarray data analysis.....	56
3.2.7 GeXP multiplex PCR	56
3.2.8 Quantitative RT-PCR.....	59
3.3 Results.....	61
3.3.1 Gene expression profiles.....	61

3.3.2 Hierarchical clustering.....	63
3.3.3 Principal Component Analysis (PCA).....	70
3.3.4 Gene ontology analysis.....	72
3.3.5 Functional annotations clustering.....	74
3.3.6 Pathway analysis.....	75
3.3.7 Hallmarks of cancer.....	75
3.3.8 Gene expression validation by GeXP.....	77
3.3.9 Gene expression validation by RT-qPCR.....	79
3.4 Discussion.....	81
CHAPTER 4	
siRNAs targeting the MAPK signalling pathway and AML1/MTG8 fusion gene attenuate the proliferation, growth arrest, apoptosis and differentiation in <i>t(8;21)</i> leukaemia.....	92
4.1 Introduction.....	92
4.2 Methodology.....	97
4.2.1 Cell culture and siRNAs transfection.....	97
4.2.2 RNA isolation and quality control.....	98
4.2.3 Quantitative RT-PCR.....	100
4.2.4 Fluorescence activated cell sorter (FACS) analysis.....	102
4.2.5 Apoptosis detection.....	102
4.2.6 Cell cycle analysis.....	103
4.2.7 Cells viability and proliferation assay.....	103
4.2.8 Microarray experiments.....	104
4.2.9 Microarray data analysis.....	104
4.3 Results.....	106
4.3.1 RNA quality and integrity assessment.....	106

4.3.2 Optimization of siRNAs concentration	106
4.3.3 Time course of mRNA suppression levels	113
4.3.4 Gene expression profiles	118
4.3.5 Gene ontology analysis.....	127
4.3.6 RT-qPCR validating microarray data	128
4.3.7 AML1/MTG8 and MAPKs suppressions reduce the proliferation rate of <i>t(8;21)</i> cells	134
4.3.8 AML1/MTG8 and MAPKs depletions support cell cycle arrest induction.....	139
4.3.9 AML1/MTG8 suppression exerts anti-apoptosis effect while MAPKs suppressions increase apoptosis in <i>t(8;21)</i> cells	144
4.3.10 AML1/MTG8 suppression supports, while MAPKs depletions inhibit the differentiation of <i>t(8;21)</i> cells	149
4.4 Discussion.....	154
CHAPTER 5 siRNAs targeting multiple genes in apoptosis signalling pathway and AML1/MTG8 fusion gene attenuate the proliferation, growth arrest, apoptosis and differentiation in <i>t(8;21)</i> leukaemia.....	166
5.1 Introduction.....	166
5.2 Methodology.....	170
5.2.1 Cell culture and siRNAs transfection.....	170
5.2.2 RNA isolation and quality control.....	171
5.2.3 Quantitative RT-PCR.....	171
5.2.4 Fluorescence-activated cell sorter (FACS) analysis.....	172
5.2.5 Apoptosis detection.....	173
5.2.6 Cell cycle analysis.....	173
5.2.7 Cells viability and proliferation assay.....	173
5.2.8 Microarray experiments.....	173

5.2.9 Microarray data analysis.....	173
5.3 Results.....	174
5.3.1 RNA quality and integrity assessment.....	174
5.3.2 Optimization of siRNAs concentration.....	174
5.3.3 Time course of mRNA suppression levels.....	179
5.3.4 Gene expression profiles.....	182
5.3.5 Gene ontology analysis.....	187
5.3.6 RT-qPCR validating microarray data.....	188
5.3.7 <i>AML1/MTG8</i> and apoptosis genes (<i>BIRC2</i> , <i>RELA</i> & <i>IL1RAP</i>) suppressions reduce the proliferation rate of t(8;21) cells	192
5.3.8 <i>AML1/MTG8</i> and apoptosis genes (<i>BIRC2</i> , <i>RELA</i> & <i>IL1RAP</i>) depletions support cell cycle arrest	196
5.3.9 <i>AML1/MTG8</i> suppression exerts anti-apoptosis effect while <i>BIRC2</i> , <i>RELA</i> and <i>IL1RAP</i> suppressions increase apoptosis in t(8;21) cells.....	200
5.3.10 <i>AML1/MTG8</i> depletion supports, while <i>BIRC2</i> and <i>IL1RAP</i> depletions inhibit, whereas <i>RELA</i> depletion has no effect on the differentiation of t(8;21) cells	204
5.4 Discussion.....	208
CHAPTER 6 General discussion.....	216
CHAPTER 7 Conclusions and recommendations.....	228
REFERENCES.....	230
APPENDICES.....	297
Appendix A Cell lines, patients and control characterisation	297
Appendix B Patients consent form.....	300
Appendix C Ethical approvals.....	307
Appendix D Bioanalyzer results.....	312

Appendix E DAVID analysis.....	316
Appendix F Hallmarks of cancer.....	328
Appendix G Primers criteria.....	338
Appendix H RT-qPCR quality control.....	339
Appendix I Cell cycle results.....	350
Appendix J Apoptosis optimization and quality control.....	353
Appendix K Differentiation optimization and quality control.....	357
Appendix L List of publications.....	361

LIST OF TABLES

		Page
Table 2.1	WHO classification of AML. (Vardiman et al. 2002).....	12
Table 3.1	Gene name, accession number, product size, left sequence with universal and right sequence with universal of GeXP primers.....	58
Table 3.2	Gene name, accession number, length, sense primer and antisense primer of RT-qPCR.....	60
Table 3.3	Spearman rho correlation analysis of differentially expressed genes among patient-1, patient-2, Kasumi-1 and SKNO-1. ** $P < 0.0001$ (2-tailed).....	68
Table 3.4	Spearman rho correlation analysis of differentially expressed genes among patients and cell lines. ** $P < 0.0001$ (2-tailed).....	68
Table 3.5	Spearman rho correlation analysis of overlapping genes among patient-1, patient-2, Kasumi-1 and SKNO-1. ** $P < 0.0001$ (2-tailed).....	69
Table 3.6	Spearman rho correlation analysis of overlapping genes among patients and cell lines. ** $P < 0.0001$ (2-tailed).....	69
Table 3.7	GeXP validating microarray data.....	78

LIST OF FIGURES

		Page
Figure 2.1	(A) Transcriptional activation of <i>AML1</i> . (B) Transcriptional repression of <i>AML1/ETO</i> . (Steffen et al. 2005).....	14
Figure 2.2	Schematic presentation of MAPK, MAPKK, and MAPKKK proteins that regulate the activation of ERK, JNK, and P38 cascades. (Geest and Coffey, 2009).....	29
Figure 3.1	Venn diagram of upregulated overlapping genes in patient samples and corresponding cell lines.....	62
Figure 3.2	Venn diagram of downregulated overlapping genes in patient samples and corresponding cell lines.....	62
Figure 3.3	Hierarchical clustering of differentially expressed genes among patient samples, cell lines (Kasumi-1 and SKNO-1), and CD34 cells.....	64
Figure 3.4	Hierarchical clustering of overlapping genes among patient samples, cell lines (Kasumi-1 and SKNO-1) and CD34 cells....	65
Figure 3.5	Hierarchical clustering of overlapping genes among patient samples, cell lines (Kasumi-1, SKNO-1, AML-193 and K-562) and CD34 cells.....	66
Figure 3.6	PCA of differentially expressed genes among patient-1(Brown), patient-2 (Silver), Kasumi-1 (Blue), SKNO-1 (Green), and CD34 cells (Red).....	71
Figure 3.7	PCA of overlapping genes among patient-1(Brown), patient-2 (Silver), Kasumi-1 (Blue), SKNO-1 (Green), and CD34 cells (Red).....	71
Figure 3.8	Ten hallmarks of cancer with corresponding examples. Red colour indicates upregulated genes, while blue colour indicates downregulated genes. (Hanahan and Weinberg, 2011).....	76
Figure 3.9	RT-qPCR validation of microarray data.....	80
Figure 3.10.	RT-qPCR validation of microarray data.....	80

List of figures continued.....		Page
Figure 4.1	siRNA-MAPK1 dose-dependent suppression. Cells were electroporated with different siRNA concentrations (10 nM, 25 nM, 50 nM, and 100 nM); 24 hours later, RNAs were extracted and knockdown levels were analyzed by RT-qPCR...	108
Figure 4.2	Melting curves of MAPK1 RT-qPCR reactions.....	108
Figure 4.3	siRNA-MAP3K1 dose-dependent suppression. Cells were electroporated with different siRNA concentrations (10 nM, 25 nM, 50 nM, and 100 nM); 24 hours later, RNAs were extracted and knockdown levels were analyzed by RT-qPCR...	109
Figure 4.4	Melting curves of MAP3K1 RT-qPCR reactions.....	109
Figure 4.5	siRNA-MAPK8 dose-dependent suppression. Cells were electroporated with different siRNA concentrations (10 nM, 25 nM, 50 nM, and 100 nM); 24 hours later, RNAs were extracted and knockdown levels were analyzed by RT-qPCR...	110
Figure 4.6	Melting curves of MAPK8 RT-qPCR reactions.....	110
Figure 4.7	siRNA-MAPK14 dose-dependent suppression. Cells were electroporated with different siRNA concentration (10 nM, 25 nM, 50 nM, and 100 nM); 24 hours later, RNAs were extracted and knockdown levels were analyzed by RT-qPCR...	111
Figure 4.8	Melting curves of MAPK14 RT-qPCR reactions.....	111
Figure 4.9	siRNA-AML1/MTG8 dose-dependent suppression. Cells were electroporated with different siRNA concentrations (25 nM, 50 nM, 100 nM, and 200 nM); 24 hours later, RNAs were extracted and knockdown levels were analyzed by RT-qPCR...	112
Figure 4.10	Melting curves of AML1/MTG8 RT-qPCR reactions.....	112
Figure 4.11	Time course depletion of <i>MAPK1</i> mRNA.....	115
Figure 4.12	Time course depletion of <i>MAP3K1</i> mRNA.....	115
Figure 4.13	Time course depletion of <i>MAPK8</i> mRNA.....	116
Figure 4.14	Time course depletion of <i>MAPK14</i> mRNA.....	116
Figure 4.15	Time course depletion of <i>AML1/MTG8</i> mRNA.....	117

List of figures continued.....

	Page	
Figure 4.16	Venn diagram of upregulated (Left) and downregulated (Right) overlapping genes (Fold change ≥ 1.5) of combination siRNAs- targeted MAPK1 and AML1/MTG8 in Kasumi-1 (Left) and SKNO-1 (Right) cell lines.....	122
Figure 4.17	Venn diagram of upregulated (Left) and downregulated (Right) overlapping genes (Fold change ≥ 1.1) of combination siRNAs- targeted MAPK1 and AML1/MTG8 in Kasumi-1 (Left) and SKNO-1 (Right) cell lines.....	122
Figure 4.18	Venn diagram of upregulated (Left) and downregulated (Right) overlapping genes (Fold change ≥ 1.5) of combination siRNAs- targeted MAP3K1 and AML1/MTG8 in Kasumi-1 (Left) and SKNO-1 (Right) cell lines.....	123
Figure 4.19	Venn diagram of upregulated (Left) and downregulated (Right) overlapping genes (Fold change ≥ 1.1) of combination siRNAs- targeted MAP3K1 and AML1/MTG8 in Kasumi-1 (Left) and SKNO-1 (Right) cell lines.....	123
Figure 4.20	Venn diagram of upregulated (Left) and downregulated (Right) overlapping genes (Fold change ≥ 1.5) of combination siRNAs- targeted MAPK8 and AML1/MTG8 in Kasumi-1 (Left) and SKNO-1 (Right) cell lines.....	124
Figure 4.21	Venn diagram of upregulated (Left) and downregulated (Right) overlapping genes (Fold change ≥ 1.1) of combination siRNAs- targeted MAPK8 and AML1/MTG8 in Kasumi-1 (Left) and SKNO-1 (Right) cell lines.....	124
Figure 4.22	Venn diagram of upregulated (Left) and downregulated (Right) overlapping genes (Fold change ≥ 1.5) of combination siRNAs- targeted MAPK14 and AML1/MTG8 in Kasumi-1 (Left) and SKNO-1 (Right) cell lines.....	125
Figure 4.23	Venn diagram of upregulated (Left) and downregulated (Right) overlapping genes (Fold change ≥ 1.1) of combination siRNAs- targeted MAPK14 and AML1/MTG8 in Kasumi-1 (Left) and SKNO-1 (Right) cell lines.....	125

List of figures continued.....	Page
Figure 4.24 Venn diagram of upregulated (Left) and downregulated (Right) overlapping genes (Fold change ≥ 1.5) of siRNA-targeted AML1/MTG8 in Kasumi-1 (Left) and SKNO-1 (Right) cell lines.....	126
Figure 4.25 Venn diagram of upregulated (Left) and downregulated (Right) overlapping genes (Fold change ≥ 1.1) of siRNA-targeted AML1/MTG8 in Kasumi-1 (Left) and SKNO-1 (Right) cell lines.....	126
Figure 4.26 Validation of microarray data by RT-qPCR. Microarray fold change and RT-qPCR relative expression level ($\Delta\Delta C_T$) of MAPK1 and AML1/MTG8 combination was determined in triplicates and normalized to B2M expression. Error bars indicate standard deviations. Kasumi-1 cell line is given on the left while SKNO-1 cell line is on the right.....	131
Figure 4.27 Validation of microarray data by RT-qPCR. Microarray fold change and RT-qPCR relative expression level ($\Delta\Delta C_T$) of MAP3K1 and AML1/MTG8 combination was determined in triplicates and normalized to B2M expression. Error bars indicate standard deviations. Kasumi-1 cell line is given on the left while SKNO-1 cell line is on the right.....	131
Figure 4.28 Validation of microarray data by RT-qPCR. Microarray fold change and RT-qPCR relative expression level ($\Delta\Delta C_T$) of MAPK8 and AML1/MTG8 combination was determined in triplicates and normalized to B2M expression. Error bars indicate standard deviations. Kasumi-1 cell line is given on the left while SKNO-1 cell line is on the right.....	132
Figure 4.29 Validation of microarray data by RT-qPCR. Microarray fold change and RT-qPCR relative expression level ($\Delta\Delta C_T$) of MAPK14 and AML1/MTG8 combinations were determined in triplicates and normalized to B2M expression. Error bars indicate standard deviations. Kasumi-1 cell line is given on the left while SKNO-1 cell line is on the right.....	132
Figure 4.30 Validation of microarray data by RT-qPCR. Microarray fold change and RT-qPCR relative expression level ($\Delta\Delta C_T$) of AML1/MTG8 were determined in triplicates and normalized to B2M expression. Error bars indicate standard deviations. Kasumi-1 cell line is given on the left while SKNO-1 cell line is on the right.....	133

List of figures continued.....		Page
Figure 4.31	Effects of MAPK1, AML1/MTG8, and the combination of MAPK1 and AML1/MTG8 suppressions on the proliferation repression. Error bars indicate standard deviations of two independent experiments, each with four replicates.....	137
Figure 4.32	Effects of MAP3K1, AML1/MTG8, and the combination of MAP3K1 and AML1/MTG8 suppressions on the proliferation repression. Error bars indicate standard deviations of two independent experiments, each with four replicates.....	137
Figure 4.33	Effects of MAPK8, AML1/MTG8, and the combination of MAPK8 and AML1/MTG8 suppressions on the proliferation repression. Error bars indicate standard deviations of two independent experiments, each with four replicates.....	138
Figure 4.34	Effects of MAPK14, AML1/MTG8, and the combination of MAPK14 and AML1/MTG8 suppressions on the proliferation repression. Error bars indicate standard deviations of two independent experiments, each with four replicates.....	138
Figure 4.35	MAPK1, AML1/MTG8 and the combination of MAPK1 and AML1/MTG8 suppressions that induce growth arrest. Error bars indicate standard deviations. <i>P</i> value was determined according to student's t-test.....	142
Figure 4.36	MAP3K1, AML1/MTG8 and the combination of MAP3K1 and AML1/MTG8 suppressions that induce growth arrest. Error bars indicate standard deviations. <i>P</i> value was determined according to student's t-test.....	142
Figure 4.37	MAPK8, AML1/MTG8 and the combination of MAPK8 and AML1/MTG8 suppressions that induce growth arrest. Error bars indicate standard deviations. <i>P</i> value was determined according to student's t-test.....	143
Figure 4.38	MAPK14, AML1/MTG8 and the combination of MAPK14 and AML1/MTG8 suppressions that induce growth arrest. Error bars indicate standard deviations. <i>P</i> value was determined according to student's t-test.....	143
Figure 4.39	Effects of MAPK1, AML1/MTG8, and the combination of MAPK1 and AML1/MTG8 suppressions on the apoptosis induction/suppression. Error bars indicate standard deviations of two independent experiments, each with triplicate technical replicates. <i>P</i> value was determined according to student's t-test.....	147

List of figures continued.....		Page
Figure 4.40	Effects of MAP3K1, AML1/MTG8, and the combination of MAP3K1 and AML1/MTG8 suppressions on the apoptosis induction/suppression. Error bars indicate standard deviations of two independent experiments, each with triplicate technical replicates. <i>P</i> value was determined according to student's t-test.....	147
Figure 4.41	Effects of MAPK8, AML1/MTG8, and the combination of MAPK8 and AML1/MTG8 suppressions on the apoptosis induction/suppression. Error bars indicate standard deviations of two independent experiments, each with triplicate technical replicates. <i>P</i> value was determined according to student's t-test.....	148
Figure 4.42	Effects of MAPK14, AML1/MTG8, and the combination of MAPK14 and AML1/MTG8 suppressions on the apoptosis induction/suppression. Error bars indicate standard deviations of two independent experiments, each with triplicate technical replicates. <i>P</i> value was determined according to student's t-test.....	148
Figure 4.43	Effects of MAPK1, AML1/MTG8, and the combination of MAPK1 and AML1/MTG8 suppressions on the differentiation induction/suppression. Error bars indicate standard deviations of two independent experiments, each with triplicate technical replicates. <i>P</i> value was determined according to student's t-test.....	152
Figure 4.44	Effects of MAP3K1, AML1/MTG8, and the combination of MAP3K1 and AML1/MTG8 suppressions on the differentiation induction/suppression. Error bars indicate standard deviations of two independent experiments, each with triplicate technical replicates. <i>P</i> value was determined according to student's t-test.....	152
Figure 4.45	Effects of MAPK8, AML1/MTG8, and the combination of MAPK8 and AML1/MTG8 suppressions on the differentiation induction/suppression. Error bars indicate standard deviations of two independent experiments, each with triplicate technical replicates. <i>P</i> value was determined according to student's t-test.....	153
Figure 4.46	Effects of MAPK14, AML1/MTG8, and the combination of MAPK14 and AML1/MTG8 suppressions on the differentiation induction/suppression. Error bars indicate standard deviations of two independent experiments, each with triplicate technical replicates. <i>P</i> value was determined according to student's t-test.....	153

List of figures continued.....		Page
Figure 5.1	siRNA dose-dependent suppressed BIRC2. Cells were electroporated with different siRNA concentrations, and after 24 hrs RNAs were extracted and knockdown levels were analyzed by RT-qPCR.....	176
Figure 5.2	Melting curves of BIRC2 RT-qPCR reactions.....	176
Figure 5.3	siRNA dose-dependent suppressed RELA. Cells were electroporated with different siRNA concentrations, and after 24 hrs RNAs were extracted and knockdown levels were analyzed by RT-qPCR.....	177
Figure 5.4	Melting curves of RELA RT-qPCR reactions.....	177
Figure 5.5	Dose of 100 nM of GeneSolution siRNAs (IL1RAP-3, IL1RAP-5, IL1RAP-6 and IL1RAP-7).....	178
Figure 5.6	Melting curves of IL1RAP RT-qPCR reactions.....	178
Figure 5.7	Time course depletion of <i>BIRC2</i> mRNA.....	180
Figure 5.8	Time course depletion of <i>RELA</i> mRNA.....	180
Figure 5.9	Time course depletion of <i>IL1RAP</i> mRNA.....	181
Figure 5.10	Venn diagram of upregulated (Left) and downregulated (Right) overlapping genes (Fold change 1.5) of combination siRNAs that targeted BIRC2 and AML1/MTG8 in Kasumi-1 (Left) and SKNO-1 (Right) cell lines.....	184
Figure 5.11	Venn diagram of upregulated (Left) and downregulated (Right) overlapping genes (Fold change 1.1) of combination siRNAs that targeted BIRC2 and AML1/MTG8 in Kasumi-1 (Left) and SKNO-1 (Right) cell lines.....	184
Figure 5.12	Venn diagram of upregulated (Left) and downregulated (Right) overlapping genes (Fold change 1.5) of combination siRNAs that targeted RELA and AML1/MTG8 in Kasumi-1 (Left) and SKNO-1 (Right) cell lines.....	185
Figure 5.13	Venn diagram of upregulated (Left) and downregulated (Right) overlapping genes (Fold change 1.1) of combination siRNAs that targeted RELA and AML1/MTG8 in Kasumi-1 (Left) and SKNO-1 (Right) cell lines.....	185

List of figures continued.....		Page
Figure 5.14	Venn diagram of upregulated (Left) and downregulated (Right) overlapping genes (Fold change 1.5) of combination siRNAs that targeted IL1RAP and AML1/MTG8 in Kasumi-1 (Left) and SKNO-1 (Right) cell lines.....	186
Figure 5.15	Venn diagram of upregulated (Left) and downregulated (Right) overlapping genes (Fold change 1.1) of combination siRNAs that targeted IL1RAP and AML1/MTG8 in Kasumi-1 (Left) and SKNO-1 (Right) cell lines.....	186
Figure 5.16	Validation of microarray data by RT-qPCR. Microarray fold change and RT-qPCR relative expression levels ($\Delta\Delta C_T$) of BIRC2 and AML1/MTG8 combination were determined in triplicates and were normalized to B2M expression. Error bars indicate standard deviations. Kasumi-1 cell line is given on the left, with SKNO-1 cell line shown on the right.....	190
Figure 5.17	Validation of microarray data by RT-qPCR. Microarray fold change and RT-qPCR relative expression levels ($\Delta\Delta C_T$) of RELA and AML1/MTG8 combination were determined in triplicates and normalized to B2M expression. Error bars indicate standard deviations. Kasumi-1 cell line is given on the left, with SKNO-1 cell line shown on the right.....	190
Figure 5.18	Validation of microarray data by RT-qPCR. Microarray fold change and RT-qPCR relative expression levels ($\Delta\Delta C_T$) of IL1RAP and AML1/MTG8 combination were determined in triplicates and normalized to B2M expression. Error bars indicate standard deviations. Kasumi-1 cell line is given on the left, with SKNO-1 cell line shown on the right.....	191
Figure 5.19	Validation of microarray data by RT-qPCR. Microarray fold change and RT-qPCR relative expression levels ($\Delta\Delta C_T$) of AML1/MTG8 were determined in triplicates and normalized to B2M expression. Error bars indicate standard deviations. Kasumi-1 cell line is given on the left, with SKNO-1 cell line shown on the right.....	191
Figure 5.20	Effects of BIRC2, AML1/MTG8, and the combination of BIRC2 and AML1/MTG8 suppressions on proliferation repression. Error bars indicate standard deviations of two independent experiments, each with triplicate technical replicates.....	194

List of figures continued.....		Page
Figure 5.21	Effects of RELA, AML1/MTG8, and the combination of RELA and AML1/MTG8 suppressions on proliferation repression. Error bars indicate standard deviations of two independent experiments, each with triplicate technical replicates.....	194
Figure 5.22	Effects of IL1RAP, AML1/MTG8, and the combination of IL1RAP and AML1/MTG8 suppressions on proliferation repression. Error bars indicate standard deviations of two independent experiments, each with triplicate technical replicates.....	195
Figure 5.23	BIRC2, AML1/MTG8 and the combination of BIRC2 and AML1/MTG8 suppressions induce growth arrest. Error bars indicate standard deviations. <i>P</i> value was determined according to student's t-test.....	198
Figure 5.24	RELA, AML1/MTG8 and the combination of RELA and AML1/MTG8 suppressions induce growth arrest. Error bars indicate standard deviations. <i>P</i> value was determined according to student's t-test.....	198
Figure 5.25	IL1RAP, AML1/MTG8 and the combination of IL1RAP and AML1/MTG8 suppressions induce growth arrest. Error bars indicate standard deviations. <i>P</i> value was determined according to student's t-test.....	199
Figure 5.26	Effects of BIRC2, AML1/MTG8, and the combination of BIRC2 and AML1/MTG8 suppressions on the apoptosis induction/suppression. Error bars indicate standard deviations of two independent experiments, each with triplicate technical replicates. <i>P</i> value was determined according to student's t-test.....	202
Figure 5.27	Effects of RELA, AML1/MTG8, and the combination of RELA and AML1/MTG8 suppressions on the apoptosis induction/suppression. Error bars indicate standard deviations of two independent experiments, each with triplicate technical replicates. <i>P</i> value was determined according to student's t-test.....	202
Figure 5.28	Effects of IL1RAP, AML1/MTG8, and the combination of IL1RAP and AML1/MTG8 suppressions on the apoptosis induction/suppression. Error bars indicate standard deviations of two independent experiments, each with triplicate technical replicates. <i>P</i> value was determined according to student's t-test.....	203

List of figures continued.....		Page
Figure 5.29	Effects of BIRC2, AML1/MTG8, and the combination of BIRC2 and AML1/MTG8 suppressions on the differentiation induction/suppression. Error bars indicate standard deviations of two independent experiments, each with triplicate technical replicates. <i>P</i> value was determined according to student's t-test.....	206
Figure 5.30	Effects of RELA, AML1/MTG8, and the combination of RELA and AML1/MTG8 suppressions on the differentiation induction/suppression. Error bars indicate standard deviations of two independent experiments, each with triplicate technical replicates. <i>P</i> value was determined according to student's t-test.....	206
Figure 5.31	Effects of IL1RAP, AML1/MTG8, and the combination of IL1RAP and AML1/MTG8 suppressions on the differentiation induction/suppression. Error bars indicate standard deviations of two independent experiments, each with triplicate technical replicates. <i>P</i> value was determined according to student's t-test.....	207

LIST OF APPENDICES

		Page
A.C.1	CRC human ethical committee approval.....	307
A.C.2	USM human ethical committee approval.....	308
A.D.1	Bioanalyzer gel image. L lane indicate ladder sample with six bands, lanes 1-10 represent RNA samples with 18S rRNA, and 28S rRNA, while lanes 11-12 represent cRNA samples.....	312
A.D.2	Electropherogram of total RNA samples. Three peaks are indicated, first peak shows the lower marker while the other peaks indicate the 18S rRNA, and 28S rRNA.....	313
A.D.3	Bioanalyzer results of total RNA samples.....	314
A.D.4	Bioanalyzer results of cRNA samples.....	315
A.E.1	Biological processes of overlapping genes.....	316
A.E.2	Cellular components of overlapping genes.....	317
A.E.3	Molecular functions of overlapping genes.....	318
A.E.4	MAPKs signalling pathway of gene ontology results of overlapping genes.....	319
A.E.5	Cell cycle pathway of gene ontology results of overlapping genes..	320
A.E.6	Neurotrophin signalling pathway of gene ontology results of overlapping genes.....	321
A.E.7	Cytokine-cytokine receptor interaction of gene ontology results of overlapping genes.....	322
A.E.8	Apoptosis pathway of gene ontology results of overlapping genes..	323
A.E.9	Toll-like receptor signalling pathway of gene ontology results of overlapping genes.....	324
A.E.10	Functional annotation clustering of upregulated overlapping genes.	325
A.E.11	Functional annotation clustering of downregulated overlapping genes.....	326

	Page
List of appendices continued.....	
A.E.12 Most significant pathways of the overlapping genes.....	327
A.F.1 Genes implicated in the hallmark self sufficiency in growth signals.	328
A.F.2 Genes implicated in the hallmark insensitivity to anti-growth signals.....	329
A.F.3 Genes implicated in apoptosis hallmark.....	330
A.F.4 Genes implicated in the hallmark limitless replicative potential.....	331
A.F.5 Genes implicated in angiogenesis hallmark.....	332
A.F.6 Genes implicated in the hallmark tissue invasion and metastasis.....	333
A.F.7 Genes implicated in the hallmark abnormal metabolic processes.....	334
A.F.8 Genes implicated in the hallmark evading the immune system.....	335
A.F.9 Genes implicated in inflammation hallmark.....	336
A.F.10 Genes implicated in the hallmark chromosome instability and mutation.....	337
A.H.1 Standard curve showing the PCR efficiency and R value of <i>ARRB1</i> gene.....	339
A.H.2 Standard curve showing the PCR efficiency and R value of <i>B2M</i> gene.....	339
A.H.3 Standard curve showing the PCR efficiency and R value of <i>BAX</i> gene.....	340
A.H.4 Standard curve showing the PCR efficiency and R value of <i>BIRC2</i> gene.....	340
A.H.5 Standard curve showing the PCR efficiency and R value of <i>CDKN1A</i> gene.....	341
A.H.6 Standard curve showing the PCR efficiency and R value of <i>DAPK3</i> gene.....	341

List of appendices continued.....		Page
A.H.7	Standard curve showing the PCR efficiency and R value of <i>DUSP2</i> gene.....	342
A.H.8	Standard curve showing the PCR efficiency and R value of <i>DUSP6</i> gene.....	342
A.H.9	A.G.9 Standard curve showing the PCR efficiency and R value of <i>FCGR1A</i> gene.....	343
A.H.10	Standard curve showing the PCR efficiency and R value of <i>GADD45A</i> gene.....	343
A.H.11	Standard curve showing the PCR efficiency and R value of <i>HK3</i> gene.....	344
A.H.12	Standard curve showing the PCR efficiency and R value of <i>HSPA6</i> gene.....	344
A.H.13	Standard curve showing the PCR efficiency and R value of <i>IL1RAP</i> gene.....	345
A.H.14	Standard curve showing the PCR efficiency and R value of <i>MAPK1</i> gene.....	345
A.H.15	Standard curve showing the PCR efficiency and R value of <i>MAP3K1</i> gene.....	346
A.H.16	Standard curve showing the PCR efficiency and R value of <i>MAPK8</i> gene.....	346
A.H.17	Standard curve showing the PCR efficiency and R value of <i>MAPK14</i> gene.....	347
A.H.18	Standard curve showing the PCR efficiency and R value of <i>MKNK2</i> gene.....	347
A.H.19	Standard curve showing the PCR efficiency and R value of <i>PRKCB1</i> gene.....	348
A.H.20	Standard curve showing the PCR efficiency and R value of <i>RELA</i> gene.....	348
A.H.21	Standard curve showing the PCR efficiency and R value of <i>SPI1</i> gene.....	349

List of appendices continued.....	Page
A.I.1 Cell cycle phase distribution results of 17 tests including; (MAPK1), (MAPK1 and AML1/MTG8), (MAP3K1), (MAP3K1 and AML1/MTG8), (MAPK8), (MAPK8 and AML1/MTG8), (MAPK14), (MAPK14 and AML1/MTG8), (BIRC2), (BIRC2 and AML1/MTG8), (RELA), (RELA and AML1/MTG8), (IL1RAP), (IL1RAP and AML1/MTG8), (AML1/MTG8), (Mock), and (AllStars siRNA control) as indicated at the lower left corner of each figure.....	350
A.J.1 Optimization and quality control of apoptosis results, five figures including untreated unstained, positive FITC, positive PI, positive mix stains (FITC and PI), and untreated stained as indicated on the top of each figure.....	353
A.J.2 Apoptosis results of 17 tests including; (MAPK1), (MAPK1 and AML1/MTG8), (MAP3K1), (MAP3K1 and AML1/MTG8), (MAPK8), (MAPK8 and AML1/MTG8), (MAPK14), (MAPK14 and AML1/MTG8), (BIRC2), (BIRC2 and AML1/MTG8), (RELA), (RELA and AML1/MTG8), (IL1RAP), (IL1RAP and AML1/MTG8), (AML1/MTG8), (Mock), and (AllStars siRNA control) as indicated on the top of each figure.....	354
A.K.1 Optimization and quality control of differentiation results, three figures including untreated unstained, untreated with isotypes, and untreated positive CD34 control as indicated on the top of each figure.....	357
A.K.2 Differentiation results of 17 tests including; (MAPK1), (MAPK1 and AML1/MTG8), (MAP3K1), (MAP3K1 and AML1/MTG8), (MAPK8), (MAPK8 and AML1/MTG8), (MAPK14), (MAPK14 and AML1/MTG8), (BIRC2), (BIRC2 and AML1/MTG8), (RELA), (RELA and AML1/MTG8), (IL1RAP), (IL1RAP and AML1/MTG8), (AML1/MTG8), (Mock), and (AllStars siRNA control) as indicated on the top of each figure.....	358

LIST OF ABBREVIATIONS

%	Percent
±	Plus minus
≥	More and equal to
↑	Increased
↓	Decreased
0C	Degree celsius
ΔΔCT	Delta delta threshold cycle
1,25 D	1,25-dihydroxy vitamin D
5-Aza-CdR	5-aza 2' deoxycytidine
5-Aza-CR	5 azacytidine
AIF	Apoptosis inducing factor
AKT/PKB	Protein kinase B
AML	Acute myelogenous leukaemia
AML-M2	Acute myeloid leukaemia subtype 2
ANLL	Acute non-lymphoid leukaemia
ANOVA	Analysis of variance
APL	Acute promyelocytic leukaemia
ara-C	Cytarabine
ARRB1	Arrestin beta 1
ARRB2	Arrestin beta 2
AS2O3	Arsenic trioxide
ATCC	American type culture collection
ATRA	All trans retinoic acid
B2M	Beta-2-microglobulin
BAX	BCL2-associated X protein
Bcl-2	B-cell CLL/lymphoma 2
BIRC2	Baculoviral IAP repeat containing 2
BP	Biological processes
BSA	Bovine serum albumin
BTZ	Bortezomib
bZIP	Basic leucine zipper
C/EBP	CAAT/enhancer binding protein

CALGB	Cancer and Leukaemia Group B
CAMs	Cell adhesion molecules
CASP	Caspase
CBF	Core binding factor
CC	Cellular components
CD	Cluster of differentiation
CDC42	Cell division cycle 42
CDK	Cyclin dependent kinase
CDKN1A	Cyclin-dependent kinase inhibitor 1A
CDKN2C	Cyclin-dependent kinase inhibitor 2C
cDNA	Complementary DNA
CML	Chronic myeloid leukaemia
c-Myc	V-myc myelocytomatosis viral oncogene homolog
CO ₂	Carbon dioxide
CR	Complete remission
cRNA	Complementary RNA
CSF3R	Colony stimulating factor 3 receptor
CT	Threshold cycle
CTL	Cytotoxic T lymphocyte
CV	Coefficient of variance
CY	Cyclophosphamide
DAPK	Death-associated protein kinase
DAPK3	Death-associated protein kinase 3
DAVID	Database for Annotation, Visualization and Integrated Discovery
DFS	Disease free survival
DIABLO	Direct IAP Binding protein with low pl
DISC	Death-inducing signalling complex
DNA	Deoxyribonucleic acid
dNTP	Deoxyribonucleotide triphosphate
dsRNA	Double-stranded RNA
DUSP2	Dual specificity phosphatase 2
DUSP6	Dual specificity phosphatase 6
EGF	Epidermal growth factor

ERK	Extracellular signal regulated kinase
ETO	Eight twenty one
EVI-1	Ecotropic viral integration 1
FAB	French American British
FACS	Fluorescence activated cell sorter
FADD	Fas-associated death domain
FasL	Fas ligands
FBS	Fetal bovine serum
FCGR1A	Fc fragment of IgG, high affinity Ia, receptor
FDA	Food and drug administration
FDR	False discovery rate
FGF	Fibroblast growth factors
FISH	Fluorescence in situ hybridization
FLT3	FMS-like tyrosine kinase 3
G6PD	Glucose-6-phosphate dehydrogenase
GADD45A	Growth arrest and DNA-damage-inducible, alpha
G-CSF	Granulocyte colony stimulating factor
GEF	Guanine exchange factor
GeXP	Gene Expression Profiler
GFI1	Growth factor independence 1
GM-CSF	Granulocyte macrophage colony stimulating factor
GO	Gene ontology
GS	Gel stain
HAT	Histone acetyltransferase
HCB	Humidity control buffer
HDAC	Histone deacetylases
HGF	Hepatocyte growth factor
HIF1A	Hypoxia inducible factor
HLA	Major histocompatibility complex
HOX	Homeobox
H-RAS	V-Ha-ras Harvey rat sarcoma viral oncogene homolog
HSC	Hematopoietic stem cell
HSPA6	Heat shock 70kDa protein 6

HtrA2	High temperature requirement protein A
HYB	Hybridization buffer
IAP	Inhibitor of apoptosis
IL	Interleukin
IL8	Interleukin 8
IRAK	IL-1R associated kinase
ITD	Internal tandem duplication
JAK-STAT	Janus kinases/signal transducers and activators of transcription
JK	Juxtamembrane
JNK	C-Jun NH2-terminal kinase
KANr	Internal control gene
KEGG	Kyoto encyclopedia of genes and genomes
KLH	Keyhole limpet hemocyanin
K-RAS	V-Ki-ras2 Kirsten rat sarcoma viral oncogene homolog
LAAs	Leukaemia associated antigens
LSC	Leukaemic stem cells
Lys-Thr-Ser	KTS tripeptide
MAML1	Mastermind-like-1
MAPK	Mitogen activated protein kinases
MAPK1	Mitogen-activated protein kinase 1
MAPK14	Mitogen-activated protein kinase 14
MAPKK	MAP kinase kinase
MAPKKK	MAP kinase kinase kinase
MCL-1	Myeloid cell leukaemia sequence 1
M-CSF	Macrophage colony-stimulating factor
MDR	Minimal Residual Disease
MDS	Myelodysplastic
MEK	MAP kinase kinase
MF	Molecular function
MIAME	Minimal information about a microarray experiment
MLL	Mixed Lineage Leukaemia
MMPs	Matrix metalloproteases
mRNA	Messenger RNA

mSin3	Mammalian Sin3
MTS	(4,5-dimethylthiazol-2-yl)-5-(3-carboxymethoxyphenyl)-2-(4-sulfophenyl)-2H-tetrazolium
MYD88	Myeloid differentiation primary response gene 88
NCoR	Nuclear receptor co-repressor
NF1	Neurofibromatosis1
NF- κ B	Nuclear factor kappa light chain enhancer of activated B cells
NGF	Nerve growth factor
nM	Nanomolar
NOD-SCID	Non-obese diabetic severe combined immunodeficient
N-RAS	Neuroblastoma RAS viral (v-ras) oncogene homolog
P53	Tumor protein p53
PBS	Phosphate buffered saline
PCA	Principal Component Analysis
PDGF	Platelet derived growth factor
PEG-rHuMGDF	Pegylated recombinant human megakaryocyte growth and development factor
PGAM4	Phosphoglycerate mutase family member 4
PGE2	Prostaglandin E2
PI3K	Phosphoinositide 3-kinase
PKA	Protein kinase A
PKCA	Protein kinase C agonists
PMA	Phorbol myristate acetate
PRKC β 1	Protein kinase C beta 1
RA	Retinoic acid
RAF	V-raf-1 murine leukaemia viral oncogene homolog
RAR α	Retinoic acid receptor, alpha
RAS	Rat sarcoma
RBL2	Retinoblastoma-like 2
RCF	Relative centrifugal force
RELA	V-rel reticuloendotheliosis viral oncogene homolog A (avian)
RHD	REL homology domains
rhTPO	Recombinant human TPO

RIN	RNA integrity number
RNA	Ribonucleic acid
RNAi	RNA interference
ROS	Reactive oxygen species
RPM	Revolutions per minute
RPS6KA3	Ribosomal protein S6 kinase, 90kDa, polypeptide 3
RQI	RNA quality indicator
RT	Reverse transcriptase
RTKs	Receptor tyrosine kinases
RT-qPCR	Quantitative reverse transcription polymerase chain reactions
RUNX1	Runt-related transcription factor-1
RUNXT1	Runt-related transcription factor 1; translocated to 1 cyclin D-related
SCF	Stem cell factor
SCID	Severe combined immunodeficiency
shRNA	Small hairpin RNA
siRNA	Small interfering RNA
Smac	Second mitochondria-derived activator of caspase
SMMHC	Smooth muscle myosin heavy chain
SON	SON DNA binding protein
SPI1	Spleen focus forming virus (SFFV) proviral integration oncogene spi 1
SPSS	Statistical Package for the Social Sciences
STAT	Signal transducers and activators of transcription
TAD	Transactivation domains
TBI	Total body irradiation
TCF/LEF	T-cell factor/lymphocyte enhancer-binding factor
TCF7L2	Transcription factor 7-like 2
TGF	Transforming growth factor
TGF- β	Transforming growth factor beta 1
TK	Tyrosine kinase
TKT	Transketolase
TLR	Toll-like receptor

TNF	Tumor necrosis factor
TNF α	Tumor necrosis factor alpha
TPO	Thrombopoietin
TRADD	TNF receptor-associated death domain
TRAF2	TNF receptor associated factor 2
TRAIL	TNF-related apoptosis inducing ligand
μ l	Microliters
WHO	World Health Organization
Wif-1	Wnt inhibitory factors-1
Wnt	Wingless-type MMTV integration site family
WT1	Wilms' tumor 1

PROFIL EKSPRESI GEN DAN MODULASI LALUAN GENETIK DALAM LEUKEMIA MEILOID AKUT T(8;21)

ABSTRAK

Kebanyakan model *in vivo* dan *in vitro* telah digunakan secara meluas dalam penyelidikan untuk mengkaji analisis laluan, sasaran dan penemuan gen. Lini sel seperti Kasumi-1 dan SKNO-1 digunakan untuk mengkaji mekanisme *t(8;21)* AML1/MTG8 dalam leukemia mieloid akut subjenis-2. Namun demikian, kadang kala keputusan yang diperoleh daripada kajian *in vitro* dan *in vivo* tidak sama atau tidak sah apabila diaplikasikan pada pesakit.

Matlamat utama kajian ini adalah untuk mengkaji persamaan dan perbezaan yang terdapat pada profil ekspresi gen daripada sampel pesakit AML *t(8;21)* serta lini sel Kasumi-1 dan SKNO-1 dibandingkan dengan sel stem CD34 yang normal.

Analisis permulaan menunjukkan bahawa 34,073 gen diekspresi secara berbeza pada pesakit dan lini sel apabila dibandingkan dengan kawalan. Pekali korelasi Spearman Rho yang diperoleh di adalah sebanyak 0.451. Terdapat 6,092 gen yang bertindan (3,297 upregulated) dan (2.795 downregulated) diantara pesakit dan lini sel. Pekali korelasi Spearman Rho yang diperoleh untuk pebandingan ini adalah sebanyak 0.826.

Oleh itu, gen bertindan dipilih untuk analisis selanjutnya. Analisis itu merangkumi pengklusteran berhierarki, ontologi gen, pengklusteran anotasi fungsian dan analisis laluan menggunakan dua perisian/sofwer yang berbeza (GeneSpring v11.5 dan DAVID v6.7). Tujuan analisis ini adalah untuk mengenal pasti fungsi gen tersebut dan laluan yang terlibat.

Dua teknik pengesahan (GeXP dan RT-qPCR) digunakan untuk mengesahkan keputusan mikrosusunan. Kedua-dua teknik ini menunjukkan kesetujuan yang kuat.

Di samping itu, gen-gen yang bertindan dinilai dan beberapa contoh diberikan bagi sepuluh (10) hallmark kanser daripada cadangan Hanahan dan Weinberg, yang antaranya: kecukupan–diri dalam isyarat pertumbuhan, ketidakpekaan terhadap isyarat antipertumbuhan, pengelakan apoptosis, potensi replikasi yang terbatas, angiogenesis lestari, metastasis dan serangan / invasi tisu, laluan metabolik tidak normal, pengelakan sistem imun, inflamasi, dan ketidakstabilan kromosom dan mutasi.

Berdasarkan keputusan mikrosusunan, analisis laluan dan teknologi RNAi (siRNA), tujuh (7) gen dalam dua (2) laluan yang berbeza, iaitu (*MAPK1*, *MAP3K1*, *MAPK8* dan *MAPK14*) dalam laluan pengisyaratan MAPKs, dan (*BIRC2*, *RELA*, dan *IL1RAP*) dalam laluan apoptosis dipilih untuk kajian lanjut melalui penekanan/supresi singlet (singlet suppression) dan dalam penekanan gabungan dengan gen *AML1/MTG8* lakur dalam leukemia t(8;21) untuk mengkaji kesan terhadap proliferasi, taburan kitaran sel, apoptosis, dan pembezaannya.

Secara amnya, semua gen – senyap (silenced gene) mengurangkan kadar proliferasi sel t(8;21) dan semua gabungan meningkatkan perencatan proliferasi. Penekanan *AML1/MTG8* mengakibatkan pencegahan apoptosis, manakala penekanan singlet dan gabungan mempengaruhi proses apoptosis. Semua gen-senyap mengaruh pertumbuhan melalui penimngkatan fasa G0/G1 dan mencegah peralihan fasa G1/S. Semua gabungan penekanan kecuali *IL1RAP* dan *AML1/MTG8* meningkatkan pertumbuhan. Walaupun penekanan *AML1/MTG8* mengaruh proses pembezaan, didapati bahawa penekanan singlet daripada tujuh gen lain tidak menunjukkan kesan terhadap pembezaan aruhan, Sementara itu, semua penekanan gabungan merencanakan proses pembezaan, kecuali *RELA* dan *IL1RAP*. Gabungan dengan penekanan *AML1/MTG8* tidak mempunyai kesan.

Eksperimen mikrosusunan dilakukan sekali lagi bagi penekanan gabungan dan data mikrosusunan disahkan melalui RT-qPCR. Ontologi gen daripada data mikrosusunan termasuk setiap gabungan dilakukan untuk memahami gen yang terlibat dalam proses proliferasi, kitaran sel, apoptosis dan pembezaan.

Secara kesimpulan, data menunjukkan bahawa lini sel Kasumi-1 and SKNO-1 adalah model yang sesuai untuk mengkaji leukemia mieloid akut subjenis-2 *t(8;21)*. Tambahan pula, pengekspresian gen melampau MAPK1, MAP3K1, MAP3K1, MAPK14, BIRC2, RELA, IL1RAP, and AML1/MTG8 mengaruh pertumbuhan sel *t(8;21)* samada melalui proliferasi atau menjadi rintang terhadap proses apoptosis. Maka, gen-gen ini mungkin berpotensi untuk menjadi sasaran terapeutik untuk leukemia *t(8;21)* leukaemia seperti yang ditunjukkan dalam eksperimen siRNA.

GENE EXPRESSION PROFILE AND MODULATION OF GENETIC PATHWAYS IN ACUTE MYELOID LEUKAEMIA T(8;21)

ABSTRACT

Many *in vivo* and *in vitro* models have been widely used in experimental research in order to facilitate pathway analysis, gene targeting and further scientific discoveries. Cell lines, such as Kasumi-1 and SKNO-1, have been used to study the AML1/MTG8 mechanisms in acute myeloid leukaemia *t(8;21)*. However, in some cases, results obtained from *in vivo* and *in vitro* studies are incompatible or not valid when applied on patients.

Given the above, the primary aim of this study is to explore and identify the similarities and differences of gene expression profiles of AML *t(8;21)* patient samples and the corresponding cell lines (Kasumi-1 and SKNO-1) as compared to normal CD34 cells.

The initial analysis revealed that there were 34,073 differentially expressed genes found in patient samples and the corresponding cell lines as compared to the control cells, with a Spearman Rho correlation coefficient of 0.451 between the patient samples and cell lines. However, the 6,092 overlapping differentially expressed genes (3,297 upregulated) and (2,795 downregulated) between patient samples and the corresponding cell lines had a Spearman Rho correlation coefficient of 0.826.

These overlapping genes were then subjected to further analysis. The analysis comprised of hierarchical clustering, gene ontology and functional annotation clustering as well as pathway analysis using two different software packages (GeneSpring v11.5 and DAVID v6.7). The aim of the analysis was to identify the function of those genes and pathways implicated within.

Two validation techniques (GeXP and RT-qPCR) were performed to confirm microarray results and the findings yielded strong agreement.

Furthermore, overlapping genes were evaluated and several examples for the ten hallmarks of cancer proposed by Hanahan and Weinberg were given, namely self-sufficiency in growth signals, insensitivity to anti-growth signals, evasion of apoptosis, limitless replication potential, sustained angiogenesis, tissue invasion and metastasis, abnormal metabolic pathways, evading the immune system, inflammation, and chromosome instability and mutation.

Based on the microarray results, pathway analysis and using RNAi technology (siRNA), seven genes in two different pathways—*MAPK1*, *MAP3K1*, *MAPK8* and *MAPK14* in MAPK signalling pathway, and *BIRC2*, *RELA*, and *IL1RAP* in apoptosis pathway—were selected for further examination by singlet suppression and in combination with the fusion gene *AML1/MTG8* in *t(8;21)* leukaemia to study their effect on proliferation, cell cycle distribution, apoptosis, and differentiation.

In general, all silenced genes resulted in reduced proliferation rate of *t(8;21)* cells, whereas all the combinations enhanced the proliferation inhibition. Despite the effect of *AML1/MTG8* suppression on apoptosis prevention, singlet and combined suppression resulted in apoptosis induction. All silenced genes induced the growth arrest by increasing the G0/G1 phase and preventing the G1/S phase transition. Similarly, the combined suppression, with the exception of *IL1RAP* and *AML1/MTG8*, enhanced the growth arrest.

Singlet suppression of the seven genes showed no effect on differentiation. However, all combined suppressions with the exception of *RELA* and *AML1/MTG8* exhibited differentiation inhibition in spite of the fact that *AML1/MTG8* promotes differentiation induction.

Microarray experiments were repeated for the combined suppression and the results were once again validated by RT-qPCR. Gene ontology of microarray data was included for every combination in order to yield better understanding of the genes implicated in the previously mentioned processes.

In conclusion, previous data demonstrate that Kasumi-1 and SKNO-1 cell lines are good models for *t(8;21)* leukemic cells. Moreover, overexpression of MAPK1, MAP3K1, MAP3K1, MAPK14, BIRC2, RELA, IL1RAP, and AML1/MTG8 induce the growth of *t(8;21)* cells either by enhancing the proliferation or resistance to apoptosis, and might be potential therapeutic targets for *t(8;21)* leukaemia as shown in siRNAs targeting.

CHAPTER 1

Introduction

1.1 Background

Due to their capability of continuous proliferation, continuous cell lines derived from human cancers have become indispensable experimental tool and their use has thus gained wide popularity in cancer research.

Thus, before commencing this study, the following two questions should be highlighted:-

First, do Kasumi-1 and SKNO-1 cell lines accurately reflect the true picture of gene expression profile of acute myeloid leukaemia (AML) patients with $t(8;21)$?

Second, are deregulated pathways in Kasumi-1 and SKNO-1 parallel to those in AML patients with $t(8;21)$?

Continuous or immortalized cell lines, compared to clinical specimens, in addition to consistency and reproducibility, are much easier to manipulate, and are thus a convenient option for cancer research. These advantages obligate researchers to first establish their work on cell cultures (*in vitro*) before moving to the next level (*in vivo*) (Mehta et al., 2007).

To ensure the highest degree of result reproducibility, cell lines are cultured in flasks, in controlled environmental and nutritional conditions. Many researchers that published results of their recent leukaemia and cancer studies have focused on the gene expression profiles and their changes. In addition to the ease of maintenance and access, cell lines have offered a convenient platform for these studies, and are thus a realistic platform for overexpressing or knocking down desired genes (Mehta et al., 2010).

There are evident differences between patient samples and their corresponding cell line models because of the differences in environmental factors to which they have been exposed (Ross and Perou, 2001). Thus, in order for the results of such studies to be clinically relevant, these variations and differences need to be precisely determined.

A comprehensive study on similarities and differences of cells obtained through different means is needed in order to establish the cell line suitability for each specific study, as only then accurate results are guaranteed and the study findings can pave the way for relevant discoveries.

In leukaemia research, myeloid cell lines, such as Kasumi-1 and SKNO-1 derived from AML FAB subtype M2, have traditionally been used in studies focusing on investigation of the molecular abnormalities of $t(8;21)$ in AML (Dunne et al, 2006).

However, in order for the collected data to be correctly interpreted and corroborated, it is imperative for a cell line and its molecular features to resemble its corresponding clinical samples. The comparisons of patient samples and their equivalent cell lines can now be procured easily, in particular since the introduction of microarray technology into this field of study.

The aim of the present study was to investigate and determine the degree of similarity and identify the key differences of gene expression profiles of $t(8;21)$ AML patients and their equivalent cell lines (Kasumi-1 and SKNO-1). Moreover, the deregulated pathways in acute myeloid leukaemia were studied.

Gene expression profile and signal transduction pathway studies in cancer research revealed the existence of several deregulated pathways that control the growth of leukaemic cells that enable their continuous proliferation, survival and apoptosis resistance (Majeti et al. 2009).

In *t(8;21)* leukaemia, *AML1* gene fuses to *ETO* gene and generates the fusion gene *AML1/ETO*, which interferes with the hematopoietic transcription and thus affects several processes, including differentiation, survival, apoptosis, and proliferation (Nimer and Moore, 2004).

Based on *in vivo* and *in vitro* comparison studies, several deregulated pathways were identified. Moreover, microarray experiments revealed the existence of many differentially overlapping expressed genes in patient samples and their corresponding cell lines when compared to their normal stem cells (CD34) compartments.

Within these pathways, many genes implicated in mitogen activated protein kinase (MAPK), apoptosis, cell cycle, and AML pathways were found; thus, in addition to the fusion gene, seven genes were selected for further investigation.

1.2 Rationale of the study

Worldwide, several studies have been conducted in the field of AML cell lines and patient research. However, the present study expands on the extant knowledge in this area in several ways, as summarized below.

1- According to the literature review (PubMed), this is the first study to be conducted on AML with *t(8;21)*, which will compare the gene expression profiles of *t(8;21)* AML patient samples and their equivalent *t(8;21)* cell lines (Kasumi-1 and SKNO-1), as well as investigate the genes and pathways deregulated in *t(8;21)* leukaemia.

2- During this project, the gene expression profile of AML (in both patients and the corresponding cell lines) will be studied and compared to control CD34 cells to identify novel and secondary therapeutic targets in *t(8;21)* leukaemia.

3- Whilst the consequences of knocking down the fusion gene *AML1/MTG8* have been well documented in *t(8;21)* leukaemia, this study will, for the first time (PubMed), be investigating the roles of MAPK and apoptosis pathways in leukaemogenesis induction by targeting several genes related to MAPK and apoptosis pathways using RNA interference (RNAi).

1.3 General objective

The key objective of the present study is to study the gene expression profile of *t(8;21)* AML patients and their corresponding cell lines, as well as the deregulated pathways that initiate the leukaemogenesis.

1.3.1 Specific objectives

- 1- To study the gene expression profile of *t(8;21)* AML (in both patients and the corresponding cell lines) versus normal control cells (CD34) using oligonucleotide microarrays.
- 2- To determine previously unidentified genes and pathways deregulated in *t(8;21)* AML compared to normal control cells (CD34).
- 3- To assess and verify degree of similarity in gene expression profiles, expression levels and functional evaluation of genes and pathways deregulated in patient samples of *t(8;21)* AML and their corresponding cell lines (Kasumi-1 and SKNO-1).
- 4- To study the effect of combination targeting of siRNAs-targeted *AML1/MTG8* and *MAPK* genes (*MAPK1*, *MAP3K1*, *MAPK8* and *MAPK14*), and assess its effect on proliferation, cell cycle distribution, apoptosis, and differentiation processes.
- 5- To study the effect of combination targeting of siRNAs-targeted *AML1/MTG8* and apoptosis genes (*BIRC2*, *RELA* and *ILIRAP*), and assess its effect on proliferation, cell cycle distribution, apoptosis, and differentiation processes.

1.4 Hypothesis

In the present study, it is hypothesized that Kasumi-1 and SKNO-1 cell lines are good models for *t(8;21)* leukaemia. Moreover, in accordance to the effect of the fusion gene (*AML1/MTG8*) in promoting leukaemogenesis, it is also hypothesized that other secondary deregulated genes could also enhance the effect of the fusion gene through controlling cell proliferation, cell cycle progression, apoptosis and differentiation processes of *t(8;21)* leukaemic cells.

1.5 Outcomes of the study

- 1- Illustrating the gene expression profile of *t(8;21)* leukaemia patient samples and their corresponding cell lines (Kasumi-1 and SKNO-1).
- 2- Determining the similarities and differences between gene expression profiles and deregulated pathways of *t(8;21)* leukaemia patients samples and their equivalent cell lines.
- 3- Identifying secondary therapeutic targets that could be used in the treatment of *t(8;21)* leukaemia.
- 4- Determining the roles of MAPKs genes (*MAPK1*, *MAP3K1*, *MAPK8* and *MAP14*) in *t(8;21)* leukaemia and demonstrating their effect on cellular processes using RNAi in a combination with *AML1/MTG8* knockdown.
- 5- Establishing the roles of apoptosis genes (*BIRC2*, *RELA* and *IL1RAP*) in *t(8;21)* leukaemia and demonstrating their effect on cellular processes using RNAi in a combination with *AML1/MTG8* knockdown.

CHAPTER 2

Literature review

Acute myeloid leukaemia (AML)—also known as acute non-lymphoid leukaemia (ANLL), acute myelogenous leukaemia, and acute myeloblastic leukaemia is a heterogeneous clonal disorder of progenitor cells (blasts), characterized by the loss of ability to normally differentiate and to respond to normal regulators of proliferation.

The inhibition of myeloid differentiation results in accumulation of various stages of early myeloid differentiated cells within bone marrow, leading to replacement of normal marrow elements (leukocytes, erythrocytes, and platelets), and increased risks of fatal infection (cellulites, pneumonia, or septicaemia), excessive bleeding and organ infiltration. Other symptoms affected individuals report may include anaemia, shortness of breath, easy bruising, petechiae, and fatigue. The progression of AML is rapid, often with fatal outcomes, if no treatment is offered (Naeim et al., 2008).

2.1 Epidemiology

AML is the most common variant of acute leukaemia that primarily affects adults, and accounts for approximately 25% of leukaemia cases. Its incidence increases with age and is particularly evident in the seventh decade of patient's life (Deschler and Lübbert, 2006). Findings of previous studies in the United Kingdom indicate that approximately 42.8% of patients were older than 65 when diagnosed with this condition, while in the US in the 1975-2003 period revealed that the incidence was approximately 3.4 per 100,000 adults (Deschler and Lübbert, 2006).

Among 4498 cancer deaths recorded in 1998 in Malaysia, those due to leukaemia represented 311 or 6.9% (Lim, 2002). According to the latest report of Ministry of Health Malaysia, published in 2006, leukaemia was one of the ten most frequent cancers among males, with incidence rate of 3.6 % and 1.9% among females (MOH, 2006).

2.2 Aetiology

The aetiology of AML is not clear; however, three major environmental factors have been reported to play significant roles in the development and incidence of AML, namely chemotherapeutic agents, exposure to chemicals, and ionizing radiation (Bowen, 2006; Warner et al., 2004)

Ionizing radiation induces DNA damage in G1 and G2 cell cycle phases, leading to chromosomal breaks that may cause mutations, deletions, and translocations. Atomic bomb survivors had a greatly increased risk (20-fold or greater) of developing AML compared to unaffected population (Deschler and Lübbert, 2006).

Chemical factors, such as topoisomerase type II inhibitors and alkylating agents, have been found to increase the incidence of AML. Alkylating agents have a medium latency period of three to six years and are usually associated with previous a myelodysplastic (MDS) phase. However, topoisomerase II inhibitors have a shorter latency period and are not associated with MDS phase (Naeim et al., 2008).

Occupational exposure to petroleum products (such as benzene), insecticides, and other organic solvents, was also found to increase the risk of developing AML (Natelson, 2007).

Increased risk of developing AML has also been noted in patients with ataxia telangiectasia, Bloom syndrome and Fanconi anaemia. Similarly, the 10-fold

increase in the incidence of AML in children with Down's syndrome (Trisomy 21) was also observed compared to their healthy peers (Segel and Lichtman, 2004).

Haematological abnormalities, such as MDS, can develop into AML. According to some authors, MDS represents the first step in the progression of the disease, with frequent detectable chromosomal aberrations, including +8, -7/*del*(7q) and -5/*del*(5q) eventually leading to AML (Naeim et al., 2008).

AMLs associated with recurrent cytogenetic abnormalities, such as *t*(8;21)(q22;q22), *t*(15;17)(q11;q12), *inv*(16)(p13q22), and *11q23* have been reported. Each chromosomal abnormality results in a unique fusion gene product that plays a significant role in regulating and initiating leukaemia (Naeim et al., 2008).

2.3 Classification

At present, AML is classified according to the two most common systems—French American British (FAB) and World Health Organization (WHO).

FAB classified AML into eight groups or subtypes, M0 through to M7, whereby each subtype is given its own characterization and morphology based on cell types and degree of maturity.

M0 refers to AML with minimal evidence of myeloid differentiation, M1 corresponds to AML without differentiation, M2 to AML with differentiation, M3 refers to acute promyelocytic leukaemia (APL), M4 to acute myelomonocytic leukaemia, M5 corresponds to acute monoblastic (M5a) or monocytic (M5b) leukaemia, M6 to acute erythroid leukaemia, and M7 to acute megakaryoblastic leukaemia (Bennett et al., 1976).

Based on biology, immunophenotyping, genetic and clinical features, WHO classified AML in the following four groups: AML with recurrent genetic

abnormalities; AML with multilineage dysplasia; AML and myelodysplastic syndrome, therapy related; and AML not otherwise categorized (Table 2.1) (Vardiman et al., 2002).

Although there are many differences between adult and paediatric AML, neither FAB nor WHO have used age in their classification; however, WHO seems to be more clinically useful than FAB classification, as the system recommends using all available data (including biological, immunophenotypic, genetic, and clinical features) for a proper identification.

The two significant differences between FAB and WHO classifications should be noted here. First, WHO lowered the percentage of blasts required for AML diagnosis to at least 20% compared to the FAB-recommendation 30%. Second, regardless of the blast percentage, patients with cytogenetic abnormalities such as *t(8;21)(q22;q22)*, *t(15;17)(q22;q12)*, *t(16;16)(p13;q22)*, and *inv(16)(p13q22)* should be considered to have AML (Vardiman et al., 2002).

In 2008, WHO updated the classification to incorporate new scientific and clinical information that became available over the preceding eight years. Thus, several changes that had been considered in leukaemia and different types of neoplasm were included in the revised classification. As in the case of AML, the major changes included translocation variants such as *11q23 (ZBTB16)*, *11q13 (NuMA)*, *5q35 (NPM) or 17q11.2 (STAT5B)*, whereby WHO recommended that these should be appointed to a specific partner, as not all responded to all-trans retinoic acid (ATRA). As a result, two new categories—AML with mutated nucleophosmin (*NPM1*) and AML with mutated CCAAT/enhancer-binding protein alpha (*CEBPA*)—were included. Three new cytogenetic variants, namely AML with *t(6;9)(p23;q34)* that generates a fusion oncogene *DEK/NUP214*, AML with *inv(3)(q21q26.2)* or

t(3;3)(q21;q26.2) that generates a fusion oncogene *RPNI/EVII*, and megakaryoblastic ALM with *t(1;22)(p13;q13)* that generates a fusion oncogene *RBM15/MKL1*, were also incorporated (Zerbini et al., 2011).

Table 2.1 WHO classification of AML. (Vardiman et al., 2002)

1	<p>AML with recurrent genetic abnormalities</p> <p>(a) AML with <i>t(8;21)(q22;q22)</i>, (<i>AML1/ETO</i>)</p> <p>(b) AML with abnormal eosinophils and <i>inv(16)</i> or <i>t(16;16)</i></p> <p>(c) APL with <i>t(15;17)</i> or variants</p> <p>(d) AML with <i>11q23 (MLL)</i> abnormalities</p>
2	<p>AML with multilineage dysplasia</p> <p>(a) Following myelodysplastic syndrome or myelodysplastic/myeloproliferative disorder</p> <p>(b) Without antecedent MDS or MDS/MPD, but with dysplasia in at least 50% of cells in 2 or more myeloid lineages</p>
3	<p>AML and myelodysplastic syndrome, therapy related</p> <p>(a) Alkylating agent/radiation-related type</p> <p>(b) Topoisomerase II inhibitor-related type (some may be lymphoid)</p> <p>(c) Other types</p>
4	<p>AML not otherwise categorized</p> <p>(a) AML minimally differentiated</p> <p>(b) AML without maturation</p> <p>(c) AML with maturation</p> <p>(d) Acute myelomonocytic leukaemia</p> <p>(e) Acute monoblastic and monocytic leukaemia</p> <p>(f) Acute erythroid leukaemia (erythroid/myeloid and pure erythroleukaemia)</p> <p>(g) Acute megakaryoblastic leukaemia</p> <p>(h) Acute basophilic leukaemia</p> <p>(i) Acute panmyelosis with myelofibrosis</p> <p>(j) Myeloid sarcoma</p>

2.3.1 AML with *t(8;21)*

Following the identification of Philadelphia chromosome *t(9;22)* in chronic myeloid leukaemia (CML) in 1960, increased attention was given to the cytogenetic finding with chromosomal translocations and the subsequent effect of fusion genes (Nowell and Hungerford, 1960).

The *t(8;21)(q22;q22)* translocation is present in 10-15% of all AML cases and 40% of AML-M2 (Miyoshi et al., 1993). The *t(8;21)* generates a chimeric gene that results in a fusion protein (AML1/MTG8 or AML1/ETO8 or RUNX1/RUNXT1), initiating the leukaemogenesis process. This translocation occurs as a result of 177 amino acid of *AML1* gene—also known as runt-related transcription factor-1 (*RUNX1*) or core binding factor (*CBF*)—located on the long arm of chromosome 21 (q22) fuses to 575 amino acid of *MTG8* genes—also called eight twenty one (*ETO*) or runt-related transcription factor 1—translocated to 1 cyclin D-related (*RUNXT1*), located on the long arm of chromosome 8 (q22), therefore converting the transcript activator into transcript repressor (Nimer and Moore, 2004).

AML1-ETO protein interferes with the function of AML1 required for normal hematopoiesis by recruiting repressor complex including nuclear receptor co-repressor (NCoR), mammalian Sin3 (mSin3), and histone deacetylases (HDAC) that interact with ETO, thus negatively regulating *AML1* gene and inhibiting myeloid differentiation, while in the absence of AML1-ETO protein, AML1 binds to its target genes and recruits co-activators. The histone acetyltransferase (HAT) activity of the co-activators causes an open chromatin structure and thereby induces AML1 target genes (Figure 2.1). This process also reduces apoptosis by activating the expression of the anti-apoptosis gene *BCL-2* (Hildebrand et al., 2001; Steffen et al., 2005).

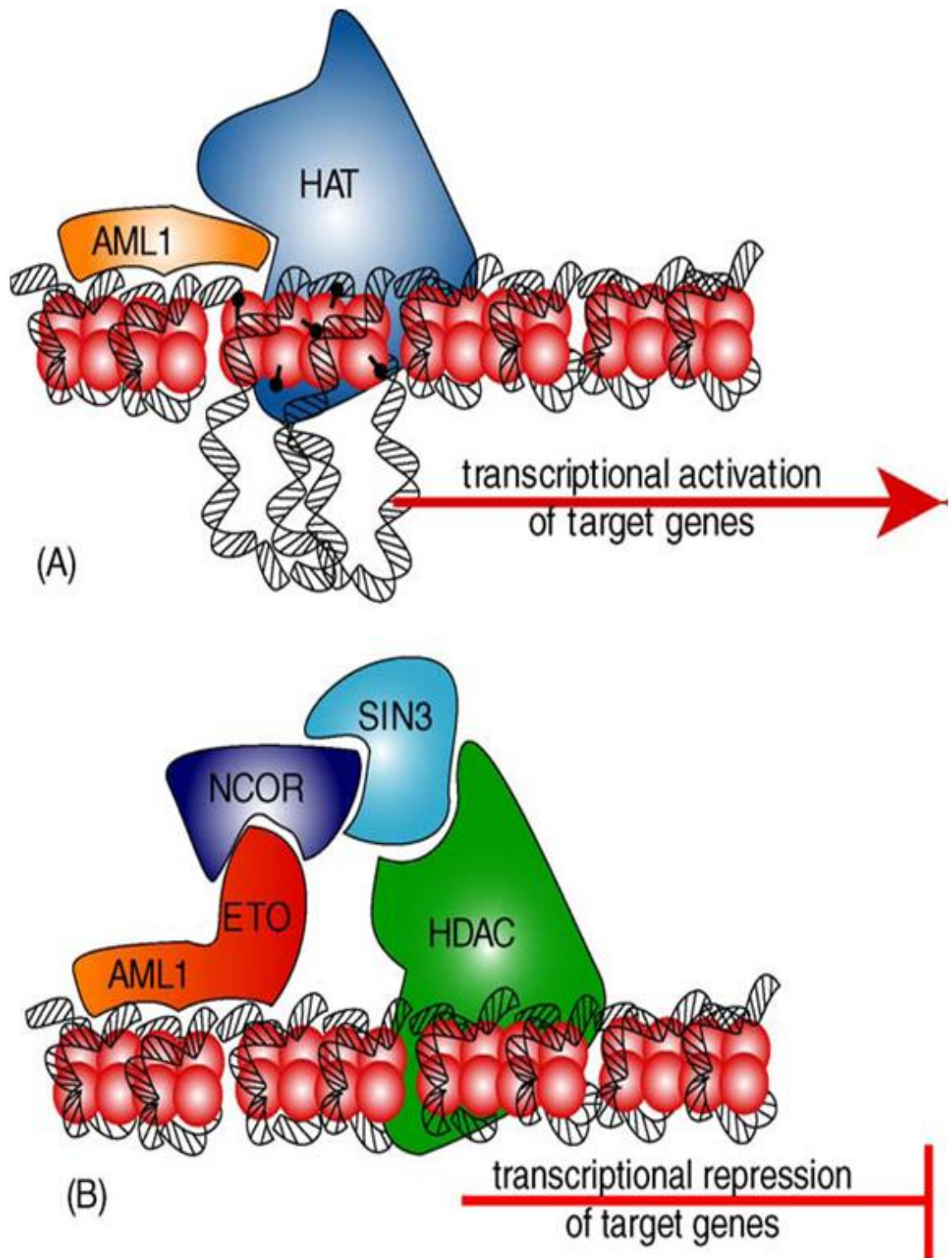


Figure 2.1 (A) Transcriptional activation of AML1. (B) Transcriptional repression of AML1/ETO. (Steffen et al., 2005)

2.3.1.1 Morphological changes and immunophenotyping

The myeloblasts are large unipotent stem cells, often with irregular nuclear shape and basophilic cytoplasm. Auer rods are frequently seen characteristic feature of myeloid blast. Promyelocytes, myelocytes, metamyelocytes, bands, and segmented neutrophils are also present and often show dysplastic changes (Naeim et al., 2008).

In a comparative study on morphological changes and cytochemistry tests between *t(8;21)* positive cells and *t(8;21)* negative cells, three main features were identified (Nakamura et al., 1997). First, homogeneous pink colour cytoplasm in mature neutrophils was identified in 90-100% of *t(8;21)* positive cells, while it was present in only 2% of *t(8;21)* negative cells. Second, pale colour cytoplasm with no granulation in mature neutrophils presented in 84% of *t(8;21)* negative cells, whereas none were identified in *t(8;21)* positive cells. Third, myeloperoxidase (MPO) was observed in 34% in mature neutrophils of *t(8;21)* negative cells compared to only 13% of *t(8;21)* positive cells (Nakamura et al., 1997).

Flow cytometric studies revealed the expression of CD13, CD117, and CD33, suggesting that HLA-DR and CD34 are often positive, whereas CD11c and CD14 are usually negative, as a sign of losing differentiation (Heidenreich et al., 2003). Moreover, aberrant expressions of CD56 and CD19 were seen in *t(8;21)* cells (Zheng et al., 2008).

2.4 Genetic alterations in AML

2.4.1 Alterations involving transcription factors

2.4.1.1 Core Binding Factor (CBF)

CBF complex is structurally altered in many AML translocations involving *t(8;21)(q22;q22)*, *inv(16)(p13;q22)* and *t(16;16)(p13;q22)*, which together constitute 25% of AML cases (Mrózek and Bloomfield, 2008).

CBF complex has two subunits, AML1 and CBF β , whereby altered AML1 encoded on the long arm of chromosome 21 (q22) is mainly associated with AML-M2, and CBF β —which is encoded on the long arm of chromosome 16 (q22)—is mainly associated with AML-M4.

The *t(8;21)(q22;q22)* has been described previously; whereas another fusion gene has also been described, where CBF β fuses to *MYH11* located on the short arm of chromosome 16 (p13), also known as smooth muscle myosin heavy chain (*SMMHC*) gene (*CBF β -MYH11*) that can be found in the other two CBF leukaemia types—*t(16;16)(p13;q22)* and *inv(16)(p13;q22)* (Engel and Hiebert, 2010).

CBF β -MYH11 or *CBF β -SMMHC* results in fusion of the first 165 amino acids of CBF β to the C-terminal of SMMHC, where they repress transcription in association with mSin3a and HDAC8 (Durst et al., 2003).

2.4.1.2 *t(15;17)(q22;q21)/PML-RAR α*

One of the most elegant translocations, which is subject of many leukaemia research studies and is given a good prognosis, is *t(15;17)*, associated with all cases of M3 or APL.

Four types of translocations associated with APL have been recorded, of which *t(15;17)(q22;q21)* is the most common and results in chimeric protein PML-RAR α

consisting of 5' portion encoded by the *PML* on the long arm of chromosome 15 (q22) and 3' portion encoded by *RARα* on the long arm of chromosome 17 (q21). As a result of this translocation, a part of *RARα* fuses to *PML* (Grimwade et al., 2000).

Several authors have suggested that this fusion is not a sole cause of APL; however, it is sufficient to alter myeloid development, block differentiation and arrest granulocytes maturation at the promyelocyte stage (Grisolano et al., 1997).

Other fusion proteins have also been reported, albeit in very rare cases, including *NuMA-RARα*, *PLZF-RARα*, *STAT5b-RARα* and *NPM-RARα* (Zelent et al., 2001).

Retinoic acid (RA) or all-trans RA (ATRA) has been shown to induce and accelerate complete remission (CR) in APL by encouraging promyelocytes to engage to the differentiation process and undergo apoptosis (Tallman et al., 1997).

The wild type of *RARα* protein acts as a transcription factor upon binding to RA and results in transcription activation; however, in the absence of RA, *RARα* wild type binds to NCoR, SMRT, mSin3, and HDACs (co-repressor proteins), causing transcription repression (Schulman et al., 1996).

2.4.1.3 Mixed Lineage Leukaemia (*MLL*): *11q23* translocation

According to research findings, *11q23/MLL* abnormalities are associated with approximately 4% of adult and 12-16% child AML cases (Mrózek et al., 2004).

Over 30 different types of chromosomal abnormalities affecting the *MLL* gene have been discovered, mostly translocations with some deletions, insertions and inversions (Mrózek et al., 2001).

The most common translocation affecting the *MLL* gene in AML is *t(9;11)(p21;q23)* that results in the *AF9-MLL* fusion gene; other translocations and fusion genes

include *t(6;11)(q27;q23)/AF6-MLL*, *t(11;19)(q23;p13.1)/MLL-ELL*, and *t(11;19)(q23;p13.3)/MLL-MLLT1* (Braekeleer et al., 2010).

Patients with *MLL* rearrangements seem to have intermediate to poor prognosis, while a good prognosis has been recorded in those with changes in *t(9;11)(p22;q23)*. *MLL* is a highly conserved protein that controls home box gene expression through chromatin remodelling. *MLL* structure consists of several domains, whereby the N-terminus contains AT hook region that serves as a DNA binding domain at the minor groove, allowing binding of regulatory transcription factors and inducing expression of *HOX* gene. In addition, it comprises two regions, SNL1 and SNL2, mediating protein subnuclear localization and a cysteine rich motif conserved DNA enzymes methyltransferase and methyl binding domain protein-1 that regulates transcription through methylation (Ayton and Cleary, 2001).

MLL fusion proteins control the expression of *HOX* genes; this regulation appears in an incomplete manner and is responsible for immortalizing myeloid progenitor cells. Results of several microarray experimental studies supported this finding, whereby highly expressed *HOXA9*, *HOXA5*, and *HOXA4* were found in many types of leukaemia associated with *MLL* translocations (Ferrando et al., 2003).

2.4.1.4 C/EBP α

CCAAT/Enhancer binding protein α (C/EBP α) is characterized by basic leucine zipper (bZIP) at the C terminal region that is used for dimerization and DNA binding, and activates transcription through binding via N-terminal transactivation domains (TADs) (Friedman and McKnight, 1990).

Although *C/EBP α* mutations have been observed in nearly 10% of AML cases, they predominantly occur in AML M1 and M2 (Pabst et al., 2001).

Two types of *C/EBP α* mutation have been shown to block AML differentiation. The first mutation is found at the bZIP that disrupts DNA binding and results in complete loss of *c/EBP α* function (Preudhomme et al., 2002). The second mutation is found at the N-terminal region and results in synthesis and translation of 30-kDa isoform of *C/EBP α* only, rather than the entire 42-kDa isoform, leading to inhibition of normal *C/EBP α* function (Pabst et al., 2001). This type of mutation seems to have a more favourable prognosis compared to the first mutation (Fröhling et al., 2004).

AML-ETO interacts with *C/EBP α* , leading to the inhibition of its function and thus inhibiting granulocyte differentiation (Pabst et al., 2001). The two additional *C/EBP α* functions are, (1) a tumour suppressor protein, whereby it inhibits cell proliferation through the activation of *p21* gene (Wang et al., 2001b; Timchenko et al., 1996), and inhibits E2F pathway leading to c-Myc inhibition thus inhibits cell proliferation (Johansen et al., 2001), and (2) a negative regulator of cell cycle through binding and inhibiting the function of CDK2 and CDK4 (Wang et al., 2001b; Wang et al., 2003).

2.4.1.5 PU.1

PU.1 is encoded by the *SPI1* gene. It encodes an ETS domain transcription factor that is required for both myeloid and lymphoid development. *PU.1* mutations have been observed in nearly 7% of AML cases; however, the mechanism through which it contributes to leukaemogenesis is still not fully understood (Mueller et al., 2002).

Homozygous mice with *PU.1* deletion developed AML within six months (Rosenbauer et al., 2004), while deletion in one *PU.1* allele and point mutation in the other allele was seen in radiation-induced murine AML (Cook et al., 2004).

PU.1 is also regulated by other transcription factors (CBF and C/EBP α), whereby it was suggested that inhibition of these transcription factors may contribute to AML by inhibiting PU.1 (Vangala et al., 2003).

2.4.1.6 *HOX* genes

Homeobox (*HOX*) genes—including A, B, C, and D clusters—encode transcription factors and play vital roles in regulating hematopoiesis. *HOX* genes control transcription activation through their DNA binding in cooperation with Pbx or Meis cofactors (Knoepfler et al., 2001).

HOXA9 has been found highly expressed in progenitor cells, downregulated through the differentiation development, and absent in mature cells (Dorsam et al., 2004). The association between *HOX* genes and leukaemogenesis have already been discussed above in the section on *MLL*.

2.4.1.7 *WT1*

Wilms' tumour I (*WT1*) is a zinc finger protein, normally expressed in stem cells; however, its expression is reduced during differentiation and is absent in mature cells (Ellisen et al., 2001).

WT1 has two domains, whereby C-terminus contains four zinc finger proteins and N-terminus contains proline and glutamine that exhibit a regulatory function. Depending on DNA binding domains and promoter status, transcription can be activated or repressed (Reddy and Licht, 1996; Yang et al., 2007).

Alternative splicing of *WT1*, with or without KTS tripeptide (Lys-Thr-Ser), in addition to mutations on exon 5, has been documented. Here, wild type (-Ex5/-KTS)

accelerates differentiation, while the mutant (+Ex5/+KTS) blocks the differentiation (Inoue et al., 1998; Loeb et al., 2003).

The presence of the mutant type interferes with the function of wild type, causing dysfunctional behaviours through forming heterodimers at the N-terminal. Moreover, (+Ex5/+KTS) isomers have been reported to be highly expressed in the majority of AML cases and are typically associated with poor prognosis, while point mutation has been documented in 15% of AML patients (Inoue et al., 1994; Miyagawa et al., 1999).

2.4.1.8 EVI-1

Although its function is not yet clear, Ectopic Viral Integration 1 (EVI-1) has been shown to be expressed in normal stem cells, it has been also suggested that EVI-1 might contribute to leukaemogenesis through interactions with SMAD3, leading to repression and inhibition of SMAD3 and TGF β , thus reducing myeloid proliferation (Métais and Dunbar, 2008).

EVI-1 has been observed highly expressed in nearly 10% of AML cases in the absence of chromosomal abnormalities and in 1-2% of AML in association with *3q26*, *-7/7q-* and *11q23* aberrations (Barjesteh van Waalwijk van Doorn-Khosrovani et al., 2003).

2.4.1.9 C-Myb

C-Myb is a proto-oncogene protein containing N-terminus for DNA binding and C-terminus for negative regulation function. It plays an important role in regulating hematopoiesis, where mice lacking C-Myb had been shown to suffer from reduction in blood elements (Mucenski et al., 1991), while its aberrant expression was

suggested to increase the proliferation of AML cells with poor prognosis (Ramsay and Gonda, 2008).

2.4.2 Alteration of signal transduction

Many articles as described below have demonstrated the presence of the association between deregulated signal transduction pathways and the initiation of leukaemogenesis process. Thus, in the present study the major pathways that contribute to leukaemogenesis are explored.

2.4.2.1 FLT3

FMS-like tyrosine kinase 3 (FLT3) is the most common mutated receptor tyrosine kinase (*RTKs*) that occurs in approximately 15-40% of AML instances, which makes it a favourite target for therapy. *FLT3* is highly expressed on stem cells and plays highly significant roles in both proliferation and differentiation (Ozeki et al., 2004).

Two types of mutation have been documented in AML, namely point mutation and internal tandem duplication (*ITD*). *ITD* occurs at exons 14 and 15 that encode juxtamembrane (JK) region and exon 20, encoding distal tyrosine kinase (TK) domain (Abu-Duhier et al., 2001). *ITD* mutations were seen in approximately 25-30% of AML cases (Stirewalt and Radich, 2003), with low frequency in M2 and M6, and high frequency in M3 (Kainz et al., 2002; Schnittger et al., 2002). On the other hand, point mutations in JK (Codon 835- Asp835) were only seen in 5-10% of AML instances (Thiede et al., 2002).

Other studies have showed that *FLT3 ITD* is not sufficient to cause AML, as *FLT3 ITD* transfection into murine cell line led to myeloproliferative, but not leukaemia (Kelly et al., 2002).

Aberrant *FLT3* mutations resulted in autophosphorylation and receptor constitutive activation, leading to the activation of several downstream targets (*RAS*, *ERK*, and *STAT*) (Choudhary et al., 2005; Hayakawa et al., 2000).

Patients with *FLT3 ITD* usually have poor prognosis, low survival rate and increase relapse rate in association with leukocytosis and high blast count (Kottaridis et al., 2001). The prognosis for patients affected by point mutation is also poor and is associated with leukocytosis and high blast count (Thiede et al., 2002).

Several *FLT3* inhibitors have been used to inhibit the *FLT3* signalling, such as CEP701 and PKC412. CEP701 was seen to inhibit *FLT3* with significant decrease in bone marrow and peripheral blood blasts. However, more studies are needed in order to fully understand the cytotoxicity of CEP701 (Knapper et al., 2006).

2.4.2.2 c-Kit

c-Kit is a proto-oncogene receptor that interacts with the stem cell factor (SCF) and plays a significant role in regulating hematopoiesis (Lennartsson et al., 2005).

According to the findings of several studies, two c-Kit regions have been associated with mutations, namely the activation loop and juxtamembrane region that serves as a negative regulation region (Chan et al., 2003; Nagata et al., 1995).

In line with in the discussion on *FLT3*, once the tyrosine kinase is phosphorylated, c-Kit is induced upon binding to SCF and activates downstream signals (PI3K, ERK), leading to the AML proliferation. Different *c-Kit* mutations, deletions, and insertions have been observed in 5-10% of AML cases (Gari et al., 1999), in particular the codon 816 and N822 (Beghini et al., 2000, 2002). In another study, substitution of Asp816 was seen in 6 of 17 patients and was thought to be highly associated with

CBF leukaemia, whereas another mutation was reported in exon 8 with exclusive association with *inv(16)* and *t(8;21)* (Gari et al., 1999).

2.4.2.3 RAS mutations

The *RAS* mutations are reported to occur in nearly 15-25% of AML cases, with *K-RAS* and *N-RAS* as the most two common *RAS* mutations found in haematological malignancies and a rare mutation of *H-RAS* (Byrne and Marshall, 1998).

As a result of these mutations, the conversion of active form (RAS-GTP) to inactive form (RAS-GDP) is prevented, thus RAS protein is embedded in the "ON" status, which continues activating other downstream pathways, such as RAF/MEK/ERK (Chang et al., 2003).

The clinical outcomes of leukaemic patients in whom *RAS* mutations have been identified are questionable, with some authors suggesting that AML patients with *RAS* mutations have improved survival rates (Neubauer et al., 1994; Neubauer et al., 2008), while in other studies no correlation between the two was found (Meshinchi et al., 2003).

2.4.2.4 Wnt pathway

Wnt ligands are a family of secreted glycoproteins critical in normal development, with β -catenin acting as the downstream mediator of Wnt pathway.

Upon the stimulation of Wnt pathway, β -catenin accumulates and moves forward to the nucleus, where acts together with the T-cell factor/lymphocyte enhancer-binding factor (TCF/LEF) complex to positively regulate transcript genes (*c-Myc* and *cyclin D1*) responsible for cell development and proliferation (Reya and Clevers, 2005).